Indian Journal of Pure & Applied Physics
Vol. 62, December 2024, pp. 1098-1105
DOI: 10.56042/ijpap.v62i12.9843

Crystal Growth and Characterization of an Efficient Nonlinear Optical Material: γ-Glycine Crystal

S Gracelin Juliana[a,*], P Sathishkumar[b] & S C Vella Durai[b]

[a]Department of Physics, Nazareth Margoschis College, Nazareth, Tamilnadu 628 617, India

[b]PG and Research Department of Physics, Sri Paramakalyani College, Alwarkurichi, Tenkasi, Tamilnadu 627 412, India

(Affiliated to Manonmaniam Sundaranar University, Abishekapatti, Tirunelveli, Tamilnadu 627 012, India)

Received 23 March 2024; accepted 8 November 2024

In an aqueous solution of ferrous chloride, γ - Glycine Crystal (γ-GC), an efficient nonlinear optical (NLO) material, was created. AR grade glycine and ferrous chloride in a molar ratio of 1: 0.5 were employed to grow the title sample. The lattice properties of γ-GC were determined using a single crystal X-ray diffraction method. High transmittance in the visible area and a UV-visible spectrum make γ-GC excellent for optical applications. Using a Nd:YAG laser, the produced crystal's LDT value was ascertained. The crystal's hardness was assessed using the Vickers test, and other mechanical properties were determined. The electrical properties of γ-GC were examined by measuring the dielectric constant and dielectric loss at various frequencies, and temperatures. Using TG/DTA tests to gauge the sample's thermal stability, the functional groups of the γ-GC were identified by FTIR analysis. The material also underwent SHG and LDT testing.

Keywords: Gamma-glycine; Dielectrics; Transmittance; Hardness; Extinction coefficient

1 Introduction

The simplest amino acid found in proteins, glycine (NH_2CH_2COOH), is an essential part of hormones, enzymes, and structural proteins. At normal temperature, glycine can exist in three polymorphic states: α-glycine, β-glycine, and γ-glycine (gamma-glycine). The crystal of γ-glycine is an essential NLO and piezoelectric material among them. Excellent NLO properties are a result of γ-glycine's crystallization in the non-Centro symmetric space group P32[1-3]. Due to its special physical and chemical characteristics, dipolar γ-glycine is a fantastic candidate for NLO, piezoelectric, and pyro electric applications[4,5]. Despite being the most stable form in terms of thermodynamics, the γ-glycine transforms into the α–form at high temperatures[6]. Possible sources for the development of γ-glycine crystals include aqueous solutions or gels containing additives, supersaturated solutions subjected to surfactant-based micro emulsions, and lamellar phase[7,8]. Profio *et al*. examined the selective nucleation of the α- and γ -forms of glycine using micro porous membranes[9]. According to the literature, additives including lithium chloride, potassium bromide, potassium chloride, and potassium chloride have all been utilized to create single crystals of γ-glycine[10–14]. Additionally, over the past few decades, scientists and crystal growers have reported abundant amounts of γ-glycine crystals with numerous additives, including $C_2H_3NaO_2$, $LiNO_3$, NH4Cl, KNO_3, $(NH_4)_2C_2O_4$, NaCl, and $CdCl_2$, among others, and their remarkable properties have been thoroughly investigated[15–21]. In this work, ferrous chloride was used as an addition to produce gamma-glycine crystals for the first time. Here, we provide the findings from the investigation of a number of factors, including the crystal's optical, structural, functional, thermal, mechanical, and elemental properties.

2 Experimental methods

2.1 Crystal growth of γ-GC

γ-GC has developed in an aqueous solution of ferrous chloride. Commercially available alpha-glycine of the AR grade and ferrous chloride were consumed in a 1: 0.5 molar ratio. The glycine and ferrous chloride were added to 2D water, and the mixture was thoroughly stirred for two hours. After stirring, the saturated solution was filtered. After that, the filtrate was kept in a beaker that was lined with porous paper. Delay in evaporation caused the

*Corresponding author: (E-mail: juliana@nmcp.ac.in)

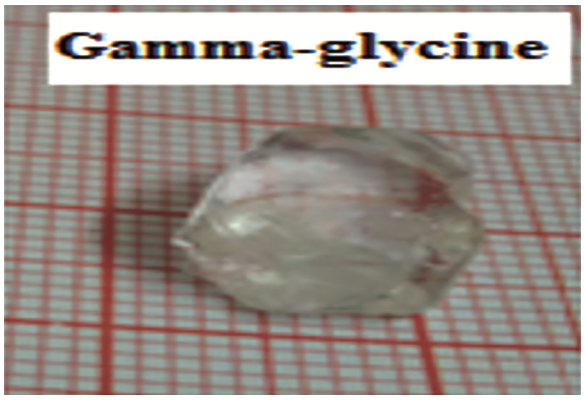

Fig. 1 — The grown of γ-GC

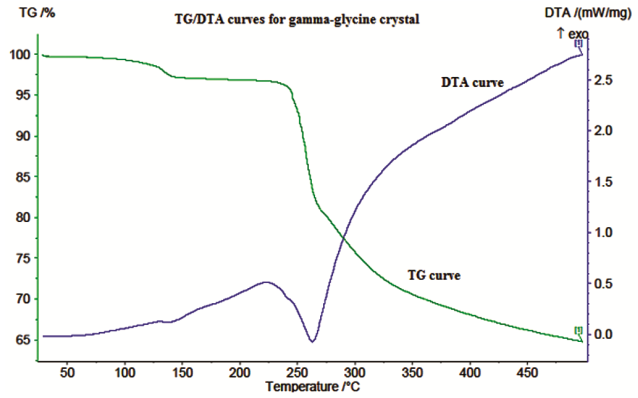

Fig. 2 — TG/DTA plot for the γ-GC

saturated solution to become supersaturated, and as it continued to evaporate, tiny crystals started to form. After approximately 30 days, the γ-GC was harvested, and a picture of the crystal is presented in Fig. 1. The γ-GC is seen to be clear and colorless.

2.2 Techniques for characterization

The grown single crystal was analyzed by single crystal XRD method using BRUKER D8 QUEST diffractometer with MoK_α radiation (λ =0.71073 Å). The crystal was examined using the SHG (Second Harmonic Generation) method with a pulsed Nd:YAG laser (Model: YG501C, λ= 1064 nm). We employed pulses with energy of 4 mJ per pulse, a pulse width of 10 ns, and a repetition rate of 10 Hz. Spectral Transmission studies were examined using a Varian Cary 5E UV-Visible-NIR spectrophotometer. A dimension of 2mm thick crystal was employed for d for the transmission studies.

Thermo gravimetric and differential thermal analyses (TG/DTA) were carried out simultaneously using a Seiko thermal analyzer in a nitrogen atmosphere and at a heating rate of 10 °C/minute for a temperature range of 25-500 °C. In order to study micro hardness of crystals, Leitz Weitzler hardness tester with a diamond indenter was used. This research was examined on a smooth, flat surface in the (001) plane of the crystal of γ-glycine. Indentations were made for a variety of loads weighing 25–125 g[22]. A multi-frequency LCR meter at different temperatures and frequencies was employed to study dielectric loss and dielectric constant of the crystal.

3 Results and discussion

3.1 Crystal structure by XRD

The XRD methods were determining the crystal structure. The crystal structure analysis was found using the single crystal XRD method. The produced

Table 1 — Unit cell parameters of γ-GC

Crystal system	Hexagonal
α	90°
β	90°
γ	120°
a (Å)	7.036(4)
b (Å)	7.036(4)
c (Å)	5.491(2)
V ($Å^3$)	235.41(2)

γ−glycine crystal's XRD data are displayed in Table 1. The results show that the γ-GC in a space group P32 hexagonal system. It is found that the sample contains 3 molecules per unit cell (Z). It is noted that the XRD results acquired in this study are in good agreement with the stated values in the literature[9].

3.2 TG/DTA studies

Figure 2 displays the thermograms from the sample's simultaneous TG/ DTA examinations at temperatures ranging from 25 to 500 °C. The γ-GC is found to be thermally stable, and it's suitable for device applications since, according to the TG curve, the γ-GC loses almost no weight up to 145 °C and only a minor amount of weight between 145 °C and 250 °C. The breakdown point for the sample, indicated by an endothermic peak on the DTA curve for the γ-GC, is at 255 °C. At temperatures between 255 and 300 °C, the sample is degrading, causing a weight loss of roughly 30%. Beyond 300 °C, the exothermic peak indicates that, the chemicals are released as gaseous products, and beyond 500 °C, the decomposition is complete.

3.3 Microhardness and other related mechanical properties

The sample's micro hardness and other important mechanical properties were examined by measuring

the micro hardness number under various loads. It is commonly known that the applied load has no bearing on a flawless crystal's hardness. Some NLO crystals are believed to exhibit both reverse indentation and conventional indentation size effects[23]. Following unloading, the d was determined by averaging the two diagonal lengths of the indentation for each applied load using the micrometre attached to the microscope eyepiece.

The Vickers microhardness number (H_v), $H_v = 1.8544\ P/\ d^2$, where P is the applied stress, and d is the average diagonal length[23]. Fig. 3 shows the hardness of γ-GC as a function of load. The findings show that as applied stress increases, the hardness value exhibits the reverse indentation size effect. The crystal surface breaks if more than 100 g of force is applied, considerably decreasing the hardness.

$P = a_1 d_1^{n1} = a_2 d_2^{n2} = a_3 d_3^{n3}$ ….. Is the general representation of Meyer's formula.

The first word could be thought of as $P = ad^n$. P stands for the load, d for the indentation's average diagonal length, 'a' for a constant, and n for the work hardening coefficient[24]. This relationship can be expressed as

$$\log_{10}(P) = \log_{10}(a) + n \log_{10}(d) \quad \text{... (1)}$$

According to sources, the value of "n" is larger than 1.6 for soft materials and less than 1.6 for hard materials, hence the γ-GC value of "n" is 2.942 and it is therefore categorized as a soft material[25]. Similar to the equation y = mx + c, where m denotes the slope and c the y-intercept, this one is a straight line. The value of "n" for γ-GC is derived from Fig. 4 to be 2.942. γ-GC is classified as a soft material because, according to reports, the value of n is greater than 1.6 for soft materials and less than 1.6 for hard materials[25].

The elastic stiffness constant (C_{11}), which also defines the kind of atomic bonds that give a material its stiffness, quantifies a substance's capacity to resist deformation. The Wooster's empirical formula[26] can be used to determine this mechanical property, which is given by the equation $C_{11} = (H_v)7/4$ and where H_v is the Vickers micro hardness. The calculated elastic constant values for γ-GC are shown in Fig. 5. Since the sample is highly rigid to deformation and the values of the elastic stiffness constant are discovered to be of the order of 10^{15}.

Utilizing the values of H_v and n, the Y of the γ-GC has been calculated. The relation utilized for $n > 2$ is provided below.

$$Y = (H_v/3) * (0.1)^{n-2} \quad \text{... (2)}$$

The relative level of resistance provided by a material without a fracture is measured by its fracture toughness (K_c), which is dependent on the circumference of the crack and the applied load and the following equation[27] is used to compute it.

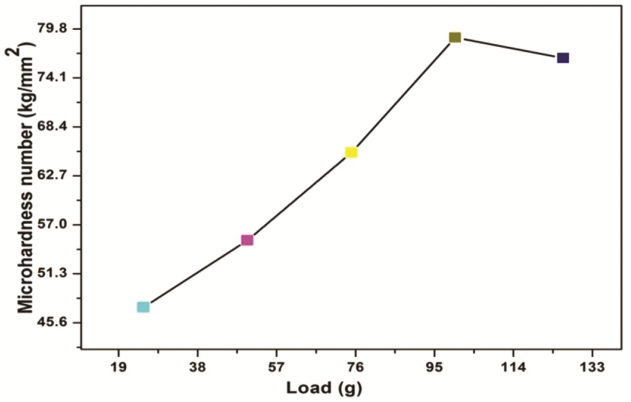

Fig. 3 — Vickers micro hardness Plot for γ-GC

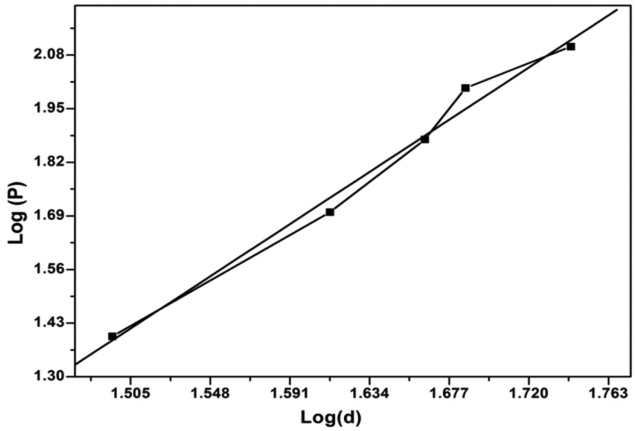

Fig. 4 — Meyer's plot of for γ-GC

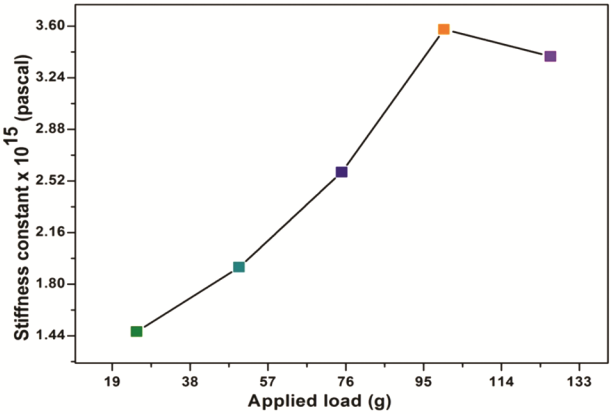

Fig. 5 — Plot of stiffness constant versus applied load for γ-GC

$$K_c = \frac{P}{\beta C^{3/2}} \quad \ldots (3)$$

Where C is the crack length from the indentation mark to the crack tip, P is the applied load and β =7 is the geometrical constant for Vickers indenter.

An essential mechanical attribute of the sample is the brittleness index (Bi), which is calculated using the following relation[28]. It is a measure of the fracture without any deformation induced in the material.

$$B_i = \frac{H_v}{K_c} \quad \ldots (4)$$

Since the applied loads of 100 g and 125 g cause fractures to form on the sample's surface, the aforementioned mechanical parameters are calculated for these two loads, and the results are shown in Table 2.

3.4 FTIR evaluation

The functional groups of a material can be identified using the FTIR spectrum. The resulting FTIR spectra are displayed in Fig. 6. The presence of the NH_3^+ stretch mode is indicated by the broad absorption peak at 3111 cm^{-1}. At 2922 and 2168 cm^{-1}, the C-H stretching frequencies are present. The existence of NH_3^+ bending and straining modes as well as the CN stretching mode, which creates the absorption band at 1126 cm^{-1}, are most likely caused by the absorption of IR frequencies at 1594 and 504 cm^{-1}. The band at 686 cm^{-1} is connected to the COO^- bending[29]. The FTIR spectrum allocations for γ-GC are shown in Table 3.

3.5 Studies on SHG

The sample's SHG efficiency can be evaluated using the Kurtz and Perry powder method[30]. Here, a pulse with a length of 6 ns and a repetition rate of 10 Hz was considered. With an input energy of 0.7 J, it was discovered that the output energy values of green radiation from KDP and γ-GC were 7.6 mJ and 9.7 mJ, respectively. A green laser beam with a 532 nm wavelength was given off by the material. Table 4 contains the information related to SHG measurement. The results show that the SHG

Table 2 — Estimated values of mechanical parameters of γ-GC

Load	Yield strength (10^6 N/m^2)	Fracture toughness ($Nm^{-3/2}$)	Brittleness Index x 10^6 ($m^{-1/2}$)
100 g	29.422	483.27	1.427
125 g	28.535	475.46	1.395

Table 3 — FTIR spectral assignments for γ-GC

Wave number (cm^{-1})	Assignments
3111	NH_3^+ stretching
2922	CH_2 stretching
2168	CH stretching
1594	NH_3^+ stretching
1498	COO^- stretching
1399	CH bending
1126	CN stretching
928	CH_2 bending
890	C-C stretching
686	COO^- wagging
504	NH_3^+ rocking

Table 4 — Values of SHG efficiency for γ-GC

Sl. No.	Sample Code / Name of the Sample	Output Energy (mille joule)	Input Energy (joule)
1	KDP (Reference)	7.6	0.70
2	γ-GC	9.7	0.70

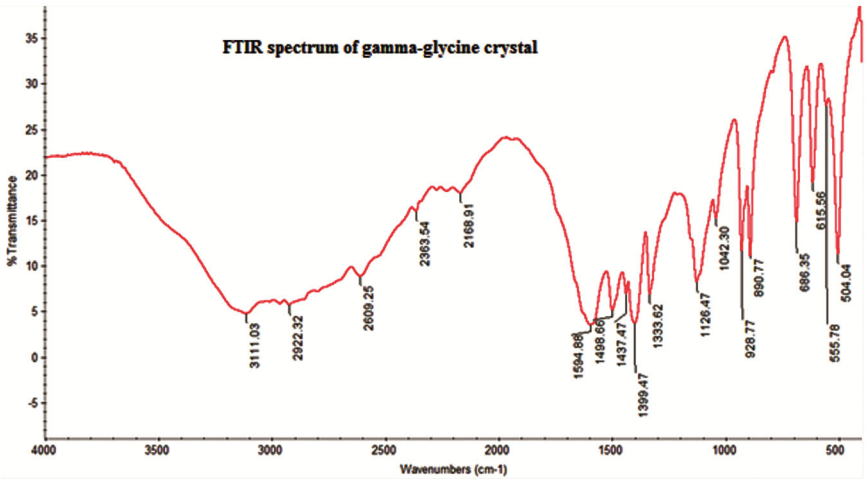

Fig. 6 — FTIR spectrum of γ-GC

efficiency of the γ-GC is 1.27 times higher than that of a conventional KDP sample.

3.6 Dielectric analysis

Each substance has a unique set of electrical qualities depending on its insulation or dielectric properties. Accurate measurement of these properties may provide information that is useful for assuring an intended usage or maintaining a proper production process. The electrical parameter for tiny signals that is most typically measured is the dielectric permittivity (ε_r), also known as the dielectric constant. To measure the dielectric, high transparency crystals were selected and used. The crystal's enlarged regions were completely removed, and the opposing faces were polished and covered with premium graphite or silver paste to create a satisfying ohmic contact. The crystal's dimensions were measured under a microscope. The dielectric constant was calculated using the formula $\varepsilon_r = C_{crys} / C_{air}$

The previously mentioned equation becomes

$$\varepsilon_r = \left(\frac{C_{crys} - C_{air}\left(1 - \frac{A_{crys}}{A_{air}}\right)}{c_{air}}\right)\left(\frac{A_{air}}{A_{crys}}\right) \quad \ldots (5)$$

where A_{crys} is the area of the crystal touching the electrode and A_{air} is the area of the electrode[31,32]. A dielectric material absorbs some of the electrical energy when an AC voltage is applied to it, and releases some of it as heat energy. This loss of electrical energy is referred to as dielectric loss. The generated crystal's AC electrical conductivity, dielectric constant and loss were measured using an Agilent (4284A) precision LCR meter with a maximum resolution of 1 mHz at varied temperatures and frequencies between 10^2 to 10^6 Hz. Fig. 7 and 8 depict variations in the γ-GC's dielectric loss and constant. According to the results, the dielectric loss and constant are significantly influenced by the temperature of the produced γ-GC and the frequency of the applied field. According to the data, loss and dielectric constant are both high at low frequencies, decrease as frequency rises, and approach virtually constant levels above 10^4 Hz. Their nature reveals the types of contributions that are involved in dielectric constant changes with frequency and temperature. When ionic and electronic polarizations are below 10^3 Hz and at high frequencies, certain materials show the dipolar orientational effect. The high dielectric constant value at low frequencies is due to space charge polarization. The sample's dielectric properties

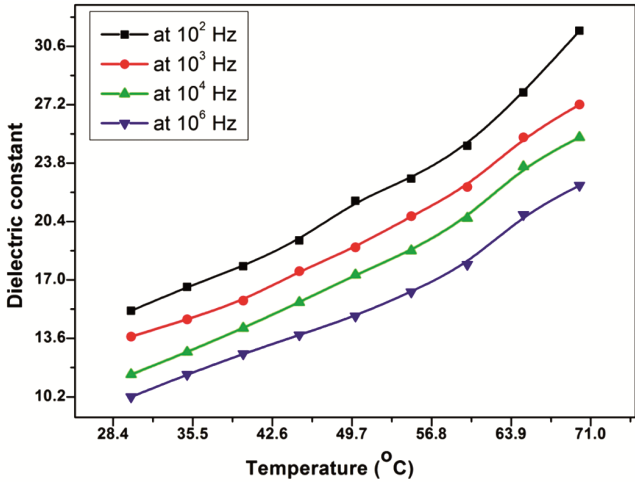

Fig. 7 — Variation of dielectric constant with temperature for γ-GC at different frequencies

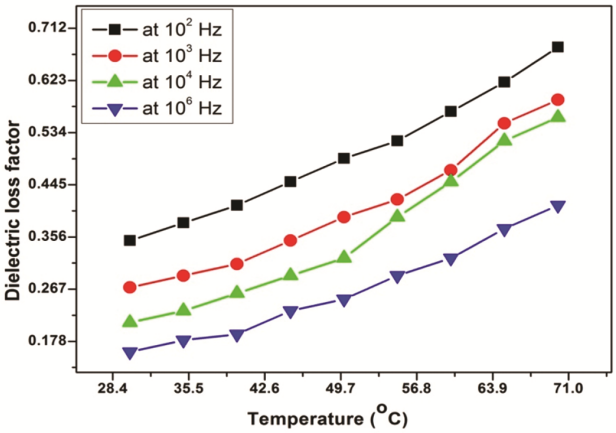

Fig. 8 — Variation of dielectric loss with temperature for γ-GC at different frequency and temperatures

are shown to increase as temperature rises for the entire frequency range (10^2 - 10^6 Hz)[33,34].

3.7 Measuring Laser Damage Threshold (LDT)

Materials must be clearly exposed to high intensity laser sources for NLO devices to work. The LDT has a considerable effect on optical applications. The ability of a material to withstand laser damage and serve as a device for NLO applications is important features and criteria in the selection of a material for NLO applications. Since nonlinear processes require high optical intensities, NLO materials must be able to with stand high power levels. The formula $P = E/\pi\tau r^2$, where E is the input energy in mJ, τ is the pulse width in ns, and r is the radius of the spot in mm, was used to get the LDT value.

The LDT value of the γ-GC was measured, and the pulse's duration was 10 ns. A convex lens has a

300 mm focal length, and there is a 150 mm gap between it and the laser. In this experiment, the crystal and lens positions were fixed, and the laser pulse's energy was increased until a discernible spot could be seen at the crystal's surface. The damage to the sample's surface may be observed by using scattered laser radiation from the sample's surface. In order to pass through the same area of damage, the laser beam and the Nd:YAG laser beam are made to be collinear. The laser damage threshold value is calculated by rapidly reducing the strength of the transmitted laser beam. Using the relationship described above, the LDT value of gamma-glycine crystal is 1.92 GW/cm^2. The standard NLO material, potassium dihydrogenphosphate (0.20 GWcm^{-2}), has a laser damage property that is nearly 9.6 times higher, and the fabrication of nonlinear optical devices may benefit from the larger value of LDT[35].

3.8 Optical research

The UV-visible transmission spectrum of the synthesized γ-GC was recorded, and the findings are shown in Fig. 9. The spectrum shows 256 nm as the UV cut-off wavelength. The sample's band gap energy was calculated to be 4.85 eV using the formula 1240 / λ. The linear absorption coefficient (α) is calculated using the relationship shown below.

$$\alpha = [2.303 \log (1/T)] / t \quad \ldots (6)$$

where T is the transmittance and t is the thickness of the sample. The value of the absorption coefficient is a crucial factor that may be used to calculate other linear optical parameters, including the optical band gap, optical conductivity, extinction coefficient, reflectance, and more. Fig. 10 shows how the absorption coefficient varies with wavelength for γ-GC, and the results show that the absorption coefficient value is low in the visible-NIR areas.

The optical band gap (E_g) of the sample can also be obtained by using the Tauc's relation given by

$$(\alpha\eta\nu)^{\nu} = A (\eta\nu - E_{\gamma}) \quad \ldots (7)$$

where E_g is the crystal's optical band gap, h is Planck's constant, α is the absorption coefficient (α) and A is a constant that varies depending on the material. In this case, n is equal to 2 for a direct band gap material while n is equal to 50% for an indirect band gap material[35]. Since n=2 is the value for which the Tauc's equation holds true, gamma-glycine is a direct band gap material. Fig. 11 illustrates the Tauc's plot between photon energy and $(\alpha\eta\nu)^2$ as a result. The optical band gap of γ-GC is 4.86 eV, as shown in the graph.

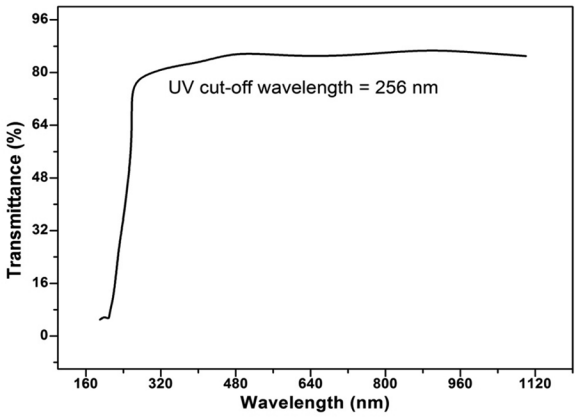

Fig. 9 — UV transmittance spectrum of γ-GC

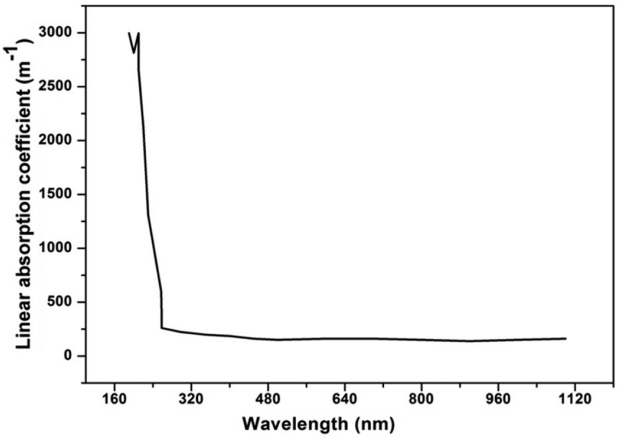

Fig. 10 — UV absorption spectra for γ-GC

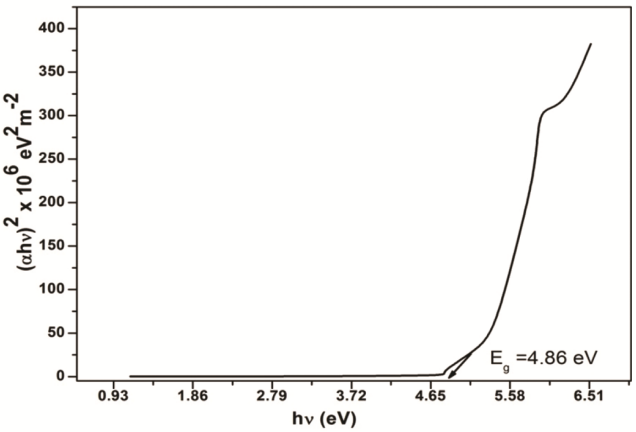

Fig. 11 — Tauc's plot for γ-GC

The extinction coefficient of γ-GC was calculated using the relation: $K = \alpha\lambda/4\pi$, where α is the linear absorption coefficient and λ is the

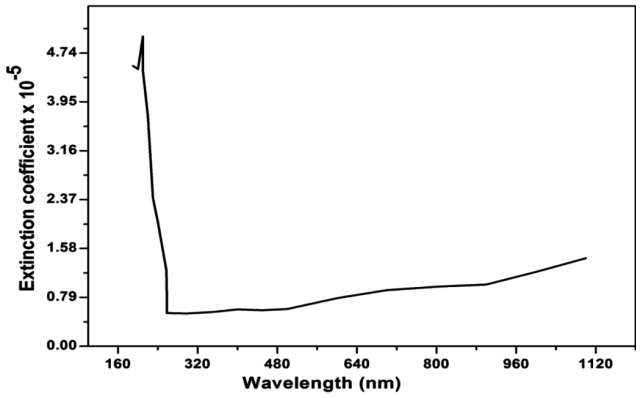

Fig. 12 — Wavelength dependence of extinction coefficient for γ-GC

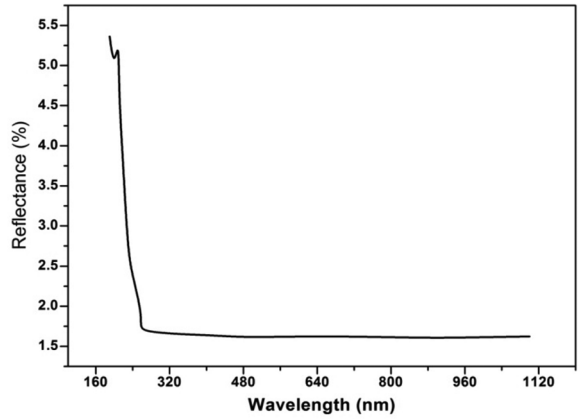

Fig. 13 — Variation of reflectance with wavelength for γ-GC

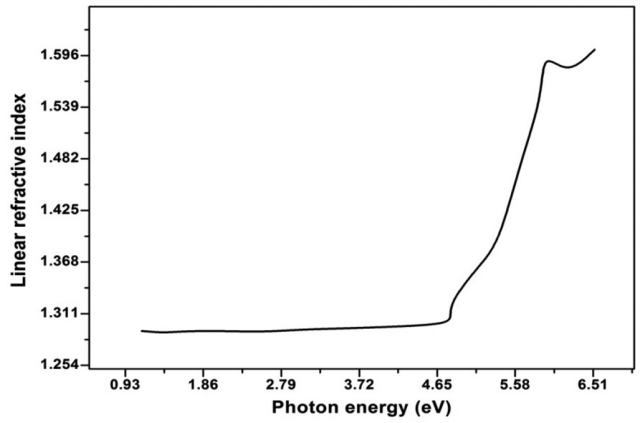

Fig. 14 — Variation of refractive index with photon energy for γ-GC

wavelength of the light. Fig. 12 depicts the plot of the wavelength dependence of the extinction coefficient for the sample. The outcome shows that the extinction coefficient rises as wavelength increases in the visible-NIR areas, but it falls off in the UV region. This sample has a low extinction value of the order of 10^{-5}, making it an excellent optical material without optical energy loss[36].

The relationship between reflectance (R), refractive index (n), and absorption coefficient (α) is given by the Fresnel formula[37].

$$R = 1 \pm \frac{\sqrt{1-\exp(-\alpha t)+\exp(\alpha t)}}{1+\exp(-\alpha t)} \quad \ldots (8)$$

Figure 13 depicts how the reflectance of a gamma-glycine crystal varies with wavelength. The linear refractive index, which measures the speed of light in a substance, is the ratio of the speed of light in a vacuum or in empty space to the speed of light in the medium. The sample's refractive index was calculated using the reflectance data and the following relationship.

$$n = \frac{1+\sqrt{R}}{1-\sqrt{R}} \quad \ldots . (9)$$

Figure 14 shows the refractive index fluctuation with photon energy for the gamma-glycine crystal. It can be seen that the refractive index is low in the visible area and high at the UV cut-off wavelength (256 nm)[38,39].

4 Conclusion

The γ-GC were grown using a slow evaporation solution growth method with alpha-glycine and ferrous chloride as the precursor ingredients. An XRD examination reveals that gamma-glycine crystallizes as hexagonal crystals. The sample is shown to be thermally stable up to 145 ^{o}C. Functional groups including NH_3^+, C-H, CN, COO^-, and others have been identified by employing FTIR analysis. It was estimated that the γ-GC has the following mechanical characteristics: brittleness index fracture toughness, hardness, work hardening coefficient, stiffness constant, and yield strength. The SHG efficiency of the γ-GC was found to be 1.27 times higher than KDP. LDT for the sample was found to be 1.92 GW/cm^2. The dielectric loss and dielectric constant values of the gamma-glycine crystal are found to be decreasing with increasing frequency and increasing with increasing temperature. We looked at the gamma-glycine crystal's transmittance, reflectance, refractive index, absorption and extinction coefficient among other linear optical parameters. The optical band gap of the sample was 4.86 eV, according to Tauc's diagram.

Acknowledgement

In order for the writers to complete this study, the staff at STIC, Cochin University (Cochin), St. Joseph's College (Trichy), Crescent Engineering College (Chennai), VIT (Vellore), NIT (Trichy), and VOC college (Tuticorin) offered valuable research**.**

References

1 Khandpekar M M & Pati S P, *Opt Commun,* 283 (2010) 2700.
2 Ferrari S, Davey R J, Cross W I, Gillon A L & Towler C S, *Cryst Growth Des*, 3 (2003) 53.
3 Yu L & Ng K, *J Pharm Sci*, 91 (2002) 2367.
4 Bhat M N & Dharmaprakash S M, *J Cryst Growth*, 242 (2002) 245.
5 Srinivasan T P, Indirajith R & Gopalakirhnan R, *J Cryst Growth*, 318 (2011) 762.
6 Zaccaro J, Matic J, Myerson A S & Garetz B A, *Cryst Growth Des*, 1 (2001) 5.
7 Allen K, Davey R J, Ferrari E, Towler C & Tiddy G J, *Cryst Growth Des*, 2 (2002) 523.
8 Towler C S, Davey R J, Lancaster R W & Price C J, *J Am Chem Soc*, 126(2004)13347.
9 Profio G D, Tucci S, Curcio E & Drioli E, *Cryst Growth Des*, 7 (2007) 526.
10 Jan B & Henryk R, *Spectrochim Acta Part A,* 61 (2005) 1611.
11 Srinivasan K, *J Cryst Growth*, 311 (2008) 156.
12 Dillip G R, Raghavaiah P & Mallikarjuna K, *Spectrochim Acta Part A*, 1 (2011) 1123.
13 Eimerl D, Velsko S, Davis L, Wang F, Loiaceono G, Kennedy G, *IEEE J Quantum Electro,* 25 (1989) 179.
14 Narayan B M & Dharmaprakash S M, *J Cryst Growth*, 242 (2002) 245.
15 Balakrishnan T, Ramesh B R & Ramamurthi K, *Spectrochim Acta PartA*, 69(2008) 1114.
16 Srinivasan T P, Indirajith R & Gopalakrishnan R, *J Cryst Growth*, 318 (2011)762.
17 Bharani raj T & Philominathan P, *J Min Mater Character Eng*, 10 (2011) 351.
18 Arputha L A, Anbuchezhiyan M, Charles K C & Selvarani K, *Mater Sci-Pol*, 35 (2017) 140.
19 Kumar Ashok, Ezhil V R, Siva kumar N, Vijayan N & Rajan B D, *Optik*, 123(2012) 409.
20 Esthaku Peter M & Ramasamy P, *Spectrochim Acta Part A*, 75 (2010) 1417.
21 Uma J & Rajendran V, *Optik*, 125(2014) 816.
22 George Vander V & Gabriel L, *Metal Progress*, 154 (1988) 21.
23 Lakshmipriya M, Babu D & Ezhil Vizhi R, *IOP Conf Ser: Mater Sci Eng*, 73 (2015) 012091.
24 Balamurugan S & Ramasamy P, *Mater Chem Phy*, 112 (2008) 1.
25 Tabor D, Blau P J & Lawn B R, (Eds.), ASTM, Philadelphia, (1985).
26 Wooster W A, *Rep Progr Phys*, 16 (1953) 62.
27 Lawn B R & Fuller E R, *J Mater Sci,* 10 (1975) 2016.
28 Nihara K, Morena R & Hasselman D P H, *J Mater Sci Lett*, 1 (1982) 13.
29 Ghazaryan V V, Fleck M & Petrosyan A M, *Spectrochim Acta Part A*, 78 (2011) 128.
30 Kurtz S K & Perry T T, *J Appl Phys*, 39 (1968) 3798.
31 Von H A, Technology Press, Cambridge, Wiley, New York, (1954).
32 Krishnan C, Selvarajan P, Freeda T H & Mahadevan C K, *Physica B*, 404 (2009)289.
33 Tareev B, Physics of dielectric materials, Mir Publishers, Moscow (1979).
34 Selvarajan P, Das B N, Gon H B & Rao K V, *J Mater Sci*, 29 (1994) 4061.
35 Sankaranarayanan K, *J Cryst Growth*, 284 (2005) 203.
36 Ashour A, El-Kadry N & Mahmoud S A, *Thin Solid Films*, 269 (1995) 117.
37 Shanthi D, Selvarajan P & Perumal S, *Optik,* 127 (2016) 3192.
38 Bhuvana K P, Robinson S J, Gopalakrishnan N & Balasubramanian T, *Mater Lett*, 61 (2007) 4246.
39 Pankove J I, Optical Processes in Semiconductors, Prentice-Hall, Englewood Cliffs, NJ, 1971.